Energy-Neutral Design Framework for Supercapacitor-Based Autonomous Wireless Sensor Networks

TRONG NHAN LE, University of Rennes 1, INRIA
ALAIN PEGATOQUET, LEAT, University of Nice, Sophia Antipolis
OLIVIER BERDER, University of Rennes 1, INRIA
OLIVIER SENTIEYS, INRIA, University of Rennes 1
ARNAUD CARER, University of Rennes 1, INRIA

To design autonomous *wireless sensor networks* (WSNs) with a theoretical infinite lifetime, *energy harvesting* (EH) techniques have been recently considered as promising approaches. Ambient sources can provide everlasting additional energy for WSN nodes and exclude their dependence on battery. In this article, an efficient energy harvesting system which is compatible with various environmental sources, such as light, heat, or wind energy, is proposed. Our platform takes advantage of double-level capacitors not only to prolong system lifetime but also to enable robust booting from the exhausting energy of the system. Simulations and experiments show that our *multiple-energy-sources converter* (MESC) can achive booting time in order of seconds. Although capacitors have virtual recharge cycles, they suffer higher leakage compared to rechargeable batteries. Increasing their size can decrease the system performance due to leakage energy. Therefore, an energy-neutral design framework providing a methodology to determine the minimum size of those storage devices satisfying *energy-neutral operation* (ENO) and maximizing system *quality-of-service* (QoS) in EH nodes, when using a given energy source, is proposed. Experiments validating this framework are performed on a real WSN platform with both photovoltaic cells and thermal generators in an indoor environment. Moreover, simulations on OMNET++ show that the energy storage optimized from our design framework is utilized up to 93.86%.

Categories and Subject Descriptors: C.2.1 [**Computer-Communication Networks**]: Network Architecture and Design—*Wireless communication*; C.4 [**Computer System Organization**]: Performance of System—*Design studies, measurement techniques*; C.5.m [**Computer System Implementation**]: Miscellaneous; I.6.5 [**Simulation and Modeling**]: Model Development—*Modeling methodologies*

General Terms: Design, Experimentation, Measurement, Performance

Additional Key Words and Phrases: Wireless sensor networks, medium access control, energy harvesting, energy neutrality, power management

ACM Reference Format:
Trong Nhan Le, Alain Pegatoquet, Olivier Berder, Olivier Sentieys, and Arnaud Carer. 2015. Energy-neutral design framework for supercapacitor-based autonomous wireless sensor networks. ACM J. Emerg. Technol. Comput. Syst. 12, 2, Article 19 (August 2015), 21 pages.
DOI: http://dx.doi.org/10.1145/2787512

This work is supported by the French National Research Agency (ANR) project GRECO bearing reference ANR-2010-SEGI-004-04.
Authors' addresses: T. N. Le (corresponding author), University of Rennes 1, 9 Rue Jean Mace, 35000 Rennes, France, INRIA; email: trong-nhan.le@unice.fr; A. Pegatoquet, LEAT, University of Nice, Sophia Antipolis, 28 Avenue Valrose, 06103 Nice, France; O. Berder, University of Rennes 1, 9 Rue Jean Mace, 35000 Rennes, France, INRIA; O. Sentieys, INRIA, University of Rennes 1, 9 Rue Jean Mace, 3500 Rennes, France; A. Carer, University of Rennes 1, 9 Rue Jean Mace, 35000 Rennes, France, INRIA.

DOI: http://dx.doi.org/10.1145/2787512

1. INTRODUCTION

Wireless sensor networks (WSNs) are designed to collect information from sensors and transmit data to a base station via wireless communications [Akyildiz et al. 2002]. Many types of sensors such as seismic, magnetic, thermal, infrared, and acoustic support various monitoring applications, ranging from home automation [Chou and Park 2005], parking guidance [Idris et al. 2009], and patient healthcare [Rincon et al. 2008] to military surveillance [He et al. 2006]. However, these applications require autonomous nodes because the battery maintenance is often impractical due to the cost and accessibility. Therefore, exploiting available environmental energy is considered as a potential solution to overcome the limited energy of batteries in a WSN node. Environmental energy can be converted from a wide range of harvesters, such as *photovoltaic* cells (PVs) [Raghunathan et al. 2005], *thermal generators* (TEGs) [Stordeur and Stark 1997], or wind turbines [Park and Chou 2006]. However, *energy harvesting* (EH) nodes need to cope with different shapes of the energy extracted from harvesters. While indoor/outdoor PVs provide high voltage but low current, TEGs output low voltage but high current. Meanwhile, wind turbines produce an AC output which also needs to be adapted.

Another challenge in EH WSNs is how to rapidly power-on the system from its empty energy state. When the system must boot from exhausted energy, it has to wait for a sufficient voltage of the storage device to power-on electronic devices. Moreover, the buffered energy must be enough for the booting process at this voltage. For a standalone storage device, if the capacity is big, it takes a long time to charge the storage device to its powered voltage level. In contrast, if the capacity is small, the charging time is reduced but it cannot store enough energy for a long period without harvesting energy. As a consequence, an efficient design consists in using double layers for the storage device. The first one, with small capacity, directly powers the whole system. The second one, with bigger capacity, is connected to the first one and allowed to be charged as soon as the first storage device reaches its regulated voltage. This structure benefits from a short charging time for the small capacity of the first storage device and is able to store a lot of energy in the second one.

Moreover, the operational lifetime of the energy storage device is an important feature when designing a long-term energy harvesting platform. Rechargeable batteries which are compatible with battery-powered WSNs can be easily used as energy storage devices. However, batteries have limited recharge cycles and sophisticated recharging circuits. Supercapacitors which have more than half a million recharge cycles and over 10-year operational lifetime are widely used in energy harvesting WSNs [Simjee and Chou 2008; Jiang et al. 2005]. Unfortunately, the leakage energy of a supercapacitor is higher than a battery [Zhu et al. 2009] and therefore needs to be properly considered in the design of a supercapacitor-based EH WSN.

Finally, the capacity of the storage device needs to be considered to provide perpetual operations, especially in a supercapacitor-based EH WSN. Instead of minimizing the consumed energy as in case of a battery-powered system, a self-powered WSN node with ambient energy adapts the consumed energy by changing its *quality-of-service* (QoS) according to the available harvested energy. For an autonomous node, it is mandatory to ensure that the consumed energy is equal to the harvested energy over a long period. This leads to *energy-neutral operation* (ENO) [Kansal et al. 2007] with an infinite system lifetime. As the harvested energy is not always available, it should be buffered in the storage device when it is, and used during the non-harvesting energy interval. If there is not sufficient space, a part of the harvested energy is discarded and degrades the average QoS. However, increasing the size of supercapacitor-based storage may not improve the QoS as the total consumed energy is increased due to leakage energy.

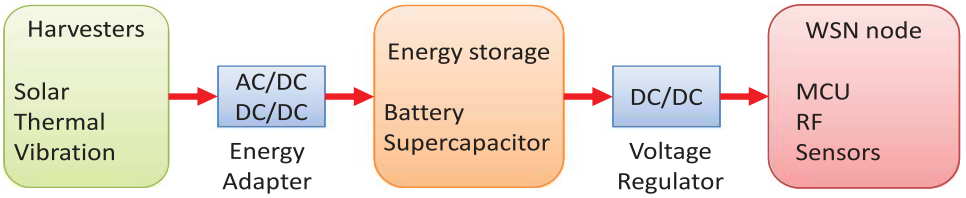

Fig. 1. Single-path architecture for EH WSN.

In this article, the first contribution is a new *multiple-energy-sources converter* (MESC) compatible with different kinds of harvesting devices such as PVs and TEGs. Our platform is simple, flexible, and easy to implement with *commercial off-the-shelf* (COTS) components. Two separate capacitors are used for energy storage to provide fast booting capability and to prolong system lifetime. While most related platforms focus on maximizing the harvested power, there are a few concerns on sizing supercapacitors, which directly impacts the system QoS due to their leakage. Therefore, a new energy-neutral design framework providing methodology to optimize the size of capacitors in MESC is also proposed as a second contribution. The objective is not only to satisfy the ENO condition but also to provide a maximum QoS according to the consumed and harvested energy.

The rest of this article is organized as follows. In Section 2, related works are presented. The hardware architecture of MESC is presented in Section 3, followed by the platform design and electrical characteristics in Section 4. Then, the energy-neutral design framework is proposed in Section 5. Experimental results with both thermal and solar energy sources used to validate our framework and optimize the size of supercapacitors are presented in Section 6. Finally, the article ends with conclusions.

2. RELATED WORK

In recent years, a large number of energy harvesting wireless sensor platforms ranging from academia to industry have been proposed. The independency of recharging or replacing batteries significantly increases the autonomy of the WSN nodes. This advantage makes the EH WSN widely used in remote places where cables are becoming impractical and costly to draw. In this section, an overview of existing platforms classified into two categories, including single-path and dual-path architectures, is presented.

2.1. Single-Path Architecture

In the traditional single-path architecture, there is only one main energy storage device, which can be a battery, a supercapacitor, or both. All the energy delivered from harvesters is used to charge the energy storage for powering the WSN node through a DC/DC converter. The energy flow for this kind of architecture is depicted in Figure 1. A *maximum-power-point tracking* (MPPT) circuit can also be integrated into the energy adapter to normalize the output energy to DC, as well as to increase the conversion efficiency. This architecture is simple and easy to implement but suffers from booting time. As the DC/DC converter requires a minimum input voltage (e.g., 1.8V with a standard DC/DC), it takes a long time to charge the empty energy storage with big capacitance to this voltage. To reduce this problem, the energy storage is usually charged to a certain voltage before deployment. Several platforms belonging to this category are described in the following.

Heliomote [Raghunathan et al. 2005] is one of the first solar EH WSN platforms. Two small PVs are directly connected to rechargeable batteries through a protection diode.

Despite its simplicity, this solution suffers some inefficiency as the harvested energy is reserved only when the output voltage from PVs is 0.7V higher than the battery voltage due to the diode drop. Moreover, as batteries have limited recharge cycles [Simjee and Chou 2008], the system lifetime is reduced to less than two years for a daily recharge. Although Heliomote is specifically designed for solar energy, the MPPT circuit is not included. To increase the conversion efficiency, two NiMH batteries are used for the energy storage whose voltage varies between 2.2V and 2.8V. Therefore, with a diode used to prevent reverse current flow into the solar panel, the output voltage of the PVs remains close to the optimal point (from 2.9V to 3.5V). A system design consideration presented in Kansal et al. [2007] provides a framework to estimate the battery size as well as the average QoS of a WSN node in the ENO mode. However, this model is only applied for a periodic solar energy source in the battery-based EH WSN.

Prometheus [Jiang et al. 2005] has a design similar to Heliomote, but with a hybrid energy storage system. It is a combination of a supercapacitor and a rechargeable battery to overcome the limited system lifetime in Raghunathan et al. [2005]. When the supercapacitor is fully charged, the surplus energy charges the battery. Otherwise, when the supercapacitor voltage is below a predefined threshold, the demanded energy is driven from the battery. By this way, the energy consumed by the WSN node is mostly served by the supercapacitor and reduces access to the battery. This solution takes advantage of more than half a million recharge cycles of a supercapacitor [Simjee and Chou 2008]. Therefore, the battery lifetime can be extended up to four years under an average of 10% load. Unfortunately, supercapacitors have higher leakage current compared to rechargeable batteries. Moreover, the larger the capacity, the greater the leakage current. Therefore, an energy model is proposed in Jiang et al. [2005] to provide a trade-off between the size of supercapacitor, the leakage energy, and the average consumed energy of a WSN node. While this energy model aims to maximize system lifetime, it does not consider the ENO condition. Prometheus also lacks a MPPT circuit and requires a high start-up voltage, which is similar to Heliomote.

Everlast [Simjee and Chou 2008] is an EH WSN platform which only uses a supercapacitor for its energy storage. By removing the battery, the system lifetime is extremely increased. Authors claim that Everlast can operate for an estimated lifetime of 20 years without any maintenance. Moreover, an MPPT is implemented by software to improve the output power from PVs. The MPPT algorithm is implemented on the microcontroller with an I-V tracer. This accurate MPPT increases the conversion efficiency of PVs up to 89%. Another improvement in Everlast is the use of a *pulse-frequency modulation* (PFM) to transfer the energy from PVs instead of directly connecting them to the energy storage. Since the supercapacitor is seen as a short circuit for the PVs when they are connected together, the voltage of PVs quickly falls to the voltage of the supercapacitor, which is usually far from the optimal operating point of PVs. By giving a series of pulses, the switch in the PFM regulator keeps the voltage of PVs around the MPP. This solution enables charging the supercapacitor up to 400% faster than direct charging, as in Heliomote or Prometheus. Unfortunately, Everlast requires a high harvested power (in order of W) due to the high-speed operations of its MPPT, and is therefore not a suitable choice for indoor harvesting systems where harvested power is only in order of mW. Finally, this work lacks a methodology for a meticulously sizing the supercapacitor.

2.2. Dual-Path Architecture

The fundamental difference between the dual-path architecture compared to the single-path one is the use of an energy flow controller. Moreover, a *primary* and a *secondary storage* (PS and SS) are used to buffer harvested energy, instead of only one storage as in the case of a single-path architecture. The main blocks of the dual-path architecture

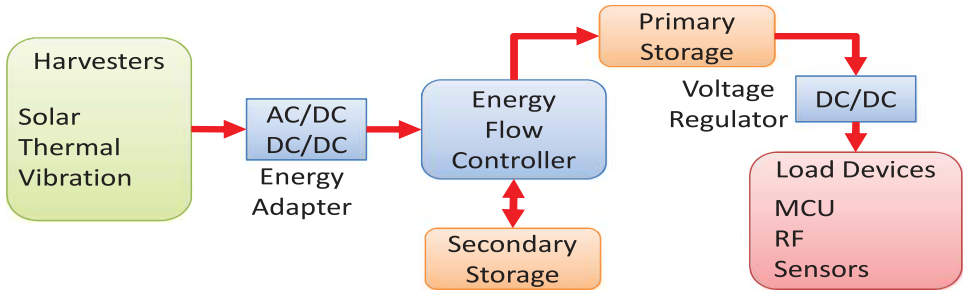

Fig. 2. Dual-path architecture for EH WSN.

are presented in Figure 2. When environmental energy is available, all harvested energy will charge the PS for powering the WSN node. As soon as the PS is fully charged, surplus energy is driven into the SS. Otherwise, when the environment energy is insufficient, the remaining energy is drawn from the SS to the PS for ensuring continuous operation of the WSN node. The advantage of this kind of architecture is a fast booting from both empty PS and SS. Due to its small capacity, PS is quickly charged to a minimum voltage that is sufficient to enable the voltage regulator, and then activates the WSN node. As SS has a big capacity, it can provide long-term operations during the period of energy absence.

DuraCap [Chen and Chou 2010] is an example of a supercapacitor-based energy storage using the dual-path architecture. This platform addresses two problems in solar-powered WSNs, including the booting process and MPPT with different PVs. Harvested energy is first used to charge a small capacitor for booting the WSN node before fulfilling an array of bigger supercapacitors. A PFM regulator and an I-V tracer similar to Prometheus are implemented to perform an MPPT function. An improvement in this platform is a bound-control circuit using a low-powered comparator to generate the control signals for the PFM regulator. The MCU is not required to be active all the time for performing MPPT in software as in Prometheus, and therefore reduces the global consumed energy. When a new PV is plugged in, the MCU temporarily disconnects it from the system to track the I-V curve. As soon as the MPP is determined, the MCU only needs to send two nonvolatile values to set the upper and lower bound for the comparator in the bound-control circuit. Then, the PFM regulator enables the new configuration to accomplish the MPPT function. This structure is extended in EscaCap [Kim and Chou 2011] with a dynamic configuration for the SS. The array of supercapacitors can be connected in series or parallel by means of a switch array. Experimental results show that EscaCap efficiently reduces the leakage energy and improves the charging speed.

As energy harvesting for a single source, especially for solar, has been well investigated, recent works deal with the combination of several sources. When considering outdoor applications, the most popular sources are solar and wind energy due to their wide availability and high power. Moreover, there seems to be a mutual complementarity between these sources: strong winds usually occur when the weather is bad rather than in sunny days, or during the night-time where solar energy is not available [Liu et al. 2010]. These reasons make solar and wind energy widely chosen in multisource platforms such as Ambimax [Park and Chou 2006] and Capnet [Ferry et al. 2013]. However, with only a single energy storage, booting time from an exhausted energy is an issue as explained in Section 2.1. Based on the dual-path architecture, a multisource and multistorage EH WSN platform is proposed in Carli et al. [2011]. A supercapacitor and a rechargeable battery are used for the PS and SS, respectively. In this work, the

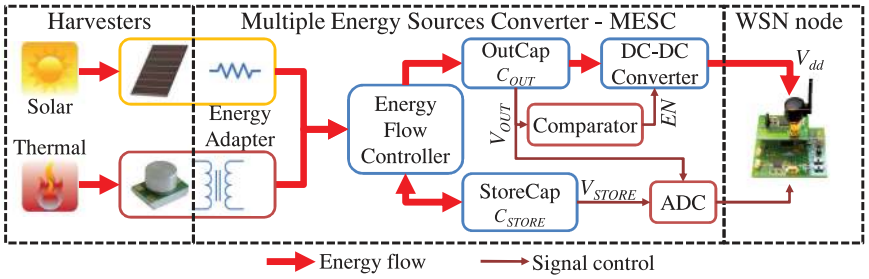

Fig. 3. MESC dual-path hardware-based architecture. The comparator enables powering the WSN node when there is sufficient energy. Both V_{OUT} and V_{STORE} are connected to the WSN through an ADC block for the *state-of-charge* (SoC) monitoring.

power management circuit acts as the energy flow controller illustrated in Figure 2. Moreover, to increase the lifetime of the battery, the charge/discharge control circuit is designed to provide overcharge and undercharge protection.

To reduce the hardware cost due to the number of external off-chip components when multiple energy sources are used, an inductor-sharing-based architecture is proposed in Bandyopadhyay and Chandrakasan [2012]. Three different harvesters are supported in this platform: PV, TEG, and piezoelectric for vibration energy. Each harvester is equipped with a power converter to normalize the output energy. Since all of these converters are designed to operate in *discontinuous conduction mode* (DCM), there is only one harvester connected to the inductor at a given time, instead of a combination of all input energy sources as proposed in Carli et al. [2011]. In this design, a switch matrix is used to reconfigure all power converters. When a converter is disconnected from the inductor, harvested energy still keeps charging its temporary capacitor. Until its schedule, energy in this capacitor is immediately transferred through the inductor to the energy storage. Therefore there is no wasted energy during the idle period of each converter.

Following these trends, we propose a *multiple-energy-sources converter* (MESC). Our aim is to provide a platform that is efficient, flexible, and easy to implement, using available COTS components. With higher efficiency, the dual-path architecture with two separate capacitors for the energy storage is applied in MESC. This structure not only provides a long system lifetime but also supports fast booting capability. However, the MPPT technique is not used in our platform because it is directly linked to a particular harvester. While PVs for solar energy have the MPP from 70% to 80% of the open circuit [Esram and Chapman 2007], TEGs for thermal energy have the MPP around 50% [Bandyopadhyay and Chandrakasan 2012]. In this work, we focus on sizing supercapacitors efficiently for the energy storage which is usually missed in related platforms. An energy-neutral design framework is proposed to optimize the storage capacity while satisfying the ENO condition and maximizing system QoS. In particular, we discuss the following issues when designing an autonomous supercapacitor-based EH WSN platform: energy storage size, harvested energy, consumed energy, and system QoS. Both periodic and continuous energy sources are considered in our design framework.

3. SYSTEM ARCHITECTURE AND OPERATION PRINCIPLES

The hardware architecture of the proposed *multiple-energy-sources converter* (MESC) is shown in Figure 3. Energy adapters are added to normalize the shape of output energy from different harvesters. For instance, PVs usually have high open circuit voltage (e.g., 5V with two PVs in series [Raghunathan et al. 2005]) to simplify the energy converter

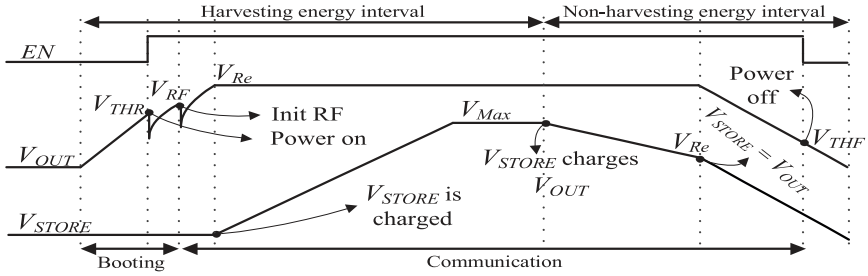

Fig. 4. System operation diagram of MESC (time and voltage are not scaled). During the harvesting energy interval, the WSN node is kept shut down until V_{OUT} reaches V_{THR}. During the non-harvesting energy interval, the WSN node is turned off when V_{OUT} decreases below V_{THF}.

with a resistor to limit the output current. Meanwhile, TEGs for thermal energy bring a very low output voltage (e.g., 20mV [Carlson et al. 2010]). In this case, a step-up transformer is added to amplify this output voltage. A combination of a diode bridge and a step-up transformer can be used for a wind generator due to its low AC-voltage output. Energy adapters should be low-powered devices to minimize power loss. For instance, Schottky diodes (BAT47) for the diode bridge [Carli et al. 2010] and Coilcraft step-up transformers (LPR6235) are dedicated to low-powered systems and can be therefore used in EH WSNs.

Two separate capacitors are used for the energy storage and are charged by the energy flow controller. The output capacitor (OutCap) is connected to a DC/DC converter to provide the voltage supply for the wireless node. The second one is a supercapacitor (StoreCap) which acts as the main energy storage. OutCap has charging priority but small capacitance compared to StoreCap. As a result, this design provides a fast booting capability due to short charging time of the small capacitor. Finally, to avoid the decreased radio range caused by decreased voltage of the OutCap, a DC/DC converter is used to provide a constant 3.3V, which is commonly compatible with WSN nodes.

Coordination of control signals to operate the system is depicted in Figure 4. At the beginning, the system is powered-off and storage devices are empty. All energy from harvesting devices first charges the OutCap. When V_{OUT} reaches the rising threshold (V_{THR}), the available energy in OutCap is sufficient for booting the system. Therefore a comparator brings the enable signal EN from low to high for powering the WSN node on. However, the available energy in the OutCap at V_{THR} is only enough for booting the system and initializing some basic modules of the microcontroller (MCU) such as I/O, Timer, and ADC. Therefore the MCU runs into sleep mode, periodically monitors V_{OUT} using a low ADC, and then initializes the radio chip until V_{OUT} reaches V_{RF}.

The energy flow controller keeps on charging OutCap to its regulated voltage (V_{Re}). After V_{OUT} has reached regulation, StoreCap is allowed to be charged. However, when V_{STORE} is charged to its maximum voltage (V_{Max}), there is no more space for harvested energy. Therefore the WSN node should utilize all harvested energy to increase the QoS and also to avoid wasting energy. When there is no more energy from harvesters (non-harvesting energy interval in Figure 4), V_{STORE} charges V_{OUT} to V_{Re} as long as V_{STORE} is still greater than V_{Re}. However, when V_{STORE} is less than V_{Re}, V_{STORE} and V_{OUT} decrease together and the system is powered-off when V_{OUT} is under the falling threshold V_{THF}.

4. PLATFORM DESIGN AND ELECTRICAL CHARACTERIZATION

To implement the harvesting energy circuit according to the block diagram proposed in Figure 3, COTS components are meticulously chosen in terms of power, footprint,

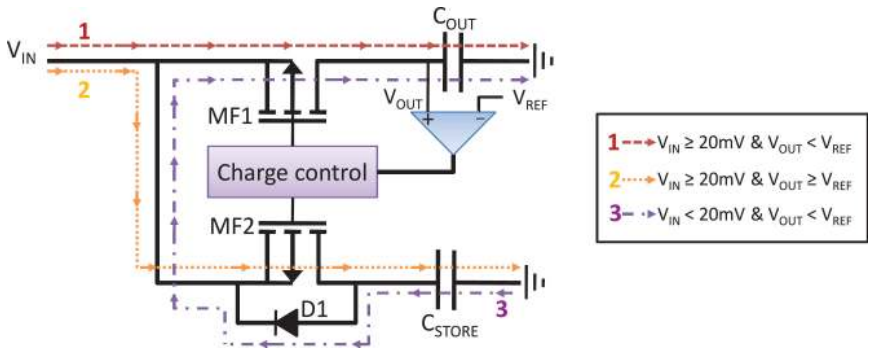

Fig. 5. Main blocks of LTC3108 with a charge control circuit and two internal mosfets providing a dual-path energy flow: when there is harvested energy ($V_{IN} \geq 20$mV), C_{OUT} is charged to its regulated voltage (1) before C_{STORE} is charged (2). When there is no more harvested energy, C_{OUT} is charged by C_{STORE} (3).

and size. The main component of MESC is the energy flow controller which provides an optimized energy flow in energy harvesting applications. *Linear Technology Company* (LTC) has proposed a wide range of ultra-low-power ICs which can be used to implement the energy flow controller. In this work, the LTC3108 component is chosen as its input voltage, ranging from 20mV to 5V, completely satisfies our requirements for indoor EH-WSNs-based applications. The dual-path energy flow is handled by a charge control and two mosfets (MF1 and MF2) as shown in Figure 5. When harvested energy is available ($V_{IN} \geq$ 20mV, the minimum input voltage) and C_{OUT} not fully charged, V_{OUT} is less than an internal V_{REF} of the LTC3108 and therefore the charge control circuit closes mosfet MF1 (on) to charge C_{OUT} first (energy flow 1 in Figure 3). As soon as V_{OUT} is higher than V_{REF}, which means C_{OUT} is fully charged, MF1 is off and MF2 is on in order to charge C_{STORE} (energy flow 2 in Figure 3). Otherwise, when harvested energy is not available, V_{OUT} is always less than V_{REF} due to the leakage and consumed energy of the WSN node, and therefore MF1 is on but MF2 is off. The energy from C_{STORE} passes through a Schottky diode D1 and charges C_{OUT} (energy flow 3 in Figure 3). More details of the LTC3108 component can be found in Salerno [2010].

The internal comparator of the LTC3108 component provides the output PGOOD signal peforming exactly the same as the EN of the comparator block in our architecture shown in Figure 3. Unfortunately, PGOOD is enabled only when V_{OUT} reaches 7% of its regulated value and is disabled when V_{OUT} drops under 9% of the regulated value. This means that, if V_{OUT} is configured to provide 3.3V, V_{THR} and V_{THR} values are 3.069V and 3.003V, respectively. This drawback requires a big capacitance for C_{OUT} to buffer sufficient energy for the booting process if PGOOD acts as the *EN* signal in Figure 3. Therefore, a nanopower MAX917 component, with rising and falling threshold that can be determined at the design phase, is used for the comparator.

Finally, a high efficiency power conversion product from *Texas Instruments* (TI) is selected for our DC/DC converter block. It is worth noting that there are two different efficiency behaviors of TI DC/DC converters. While TPS6120x provides a high efficiency at high output current (90% at 500mA) but very low efficiency at low output current (40% at 0.1mA), TPS6103x provides a low efficiency at high output current (70% at 1000mA) but very high efficiency at low output current (90% at 1mA). Therefore, in the context of EH WSNs, the TPS61030 is chosen for the DC/DC converter as the average consumed current of a WSN node is in order of mA.

A schematic overview of MESC can be found in Figure 6. The energy adapter is designed as a multichoice footprint which can be soldered by two resistors (R_3 and R_4) in case of PVs, or a step-up transformer (T_1) in case of TEGs. The falling threshold (V_{THF})

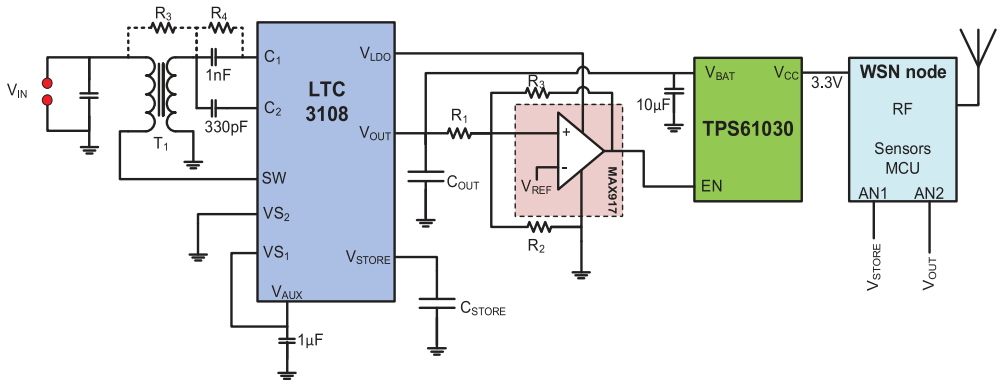

Fig. 6. Overview schematic of MESC. Either two resistors (R_3 and R_4) for PVs or a step-up transformer (T1) are used for the energy adapter. Two outputs of LTC3108 are connected to C_{OUT} and C_{STORE} while V_{LDO} is used to power the comparator MAX917, having an internal reference voltage $V_{REF} = 1.245$V. Both V_{STORE} and V_{OUT} are connected to two ADC pins of MCU (AN1 and AN2) for the SoC monitoring.

can be chosen as the minimum input voltage of the DC/DC converter, while the rising threshold (V_{THR}) is in the range of $[V_{THF}, V_{Re}]$. In the current version of MESC, R_1, R_2, and R_3 are computed to provide $V_{THF} = 1.8$V and $V_{THR} = 2.9$V. How to determine C_{OUT} and C_{STORE} in order to satisfy ENO and maximize QoS is described in the next section. The main advantage of our platform when only supercapacitors are used for the secondary energy storage, compared to other hybrid storages in Glavin et al. [2008] or Ongaro et al. [2012], is that a simple energy monitor proposed in Le et al. [2013] can be used to provide harvesting-energy-aware capability. By reading the voltage of the StoreCap and tracking all activities of the WSN node, the harvested as well as consumed energy can be estimated. A low-powered battery monitor IC in Raghunathan et al. [2005] is not required in our platform since the available energy in a supercapacitor can be easily estimated by measuring its voltage. However, besides the high leakage of supercapacitors that needs to be considered, another problem, called paradox of two charged capacitors, can occur in our platform when C_{STORE} charges C_{OUT} and therefore reduces the average efficiency. When the capacitor is directly charged without a current limiting circuit, the high charge rate of the current results in electromagnetic loss [Sommariva 2003]. This loss of energy can be up to 50% when directly charging a capacitor from another identical capacitor [Tse et al. 1995]. Fortunately, the discharged current from C_{STORE} is limited to only few milliamps in LTC3108, thus reducing the paradox problem.

The electrical characteristics of MESC, including the leakage energy and the DC/DC converter efficiency, are estimated from experimental measurements. A CapXX supercapacitor of 0.9F is used for StoreCap (C_{STORE}). At the beginning of the measurement, V_{STORE} is 4.925V and the WSN node is disconnected from MESC. Due to the leakage energy, V_{STORE} is linearly reduced to 4.825V after 10000s. Therefore the total leakage energy for a period T can be estimated by

$$E_{Leak} = P_{Leak} T, \tag{1}$$

where P_{Leak} is the leakage power defined as

$$P_{Leak} = \frac{1}{2}(0.9F)\frac{(4.925V)^2 - (4.825V)^2}{(10000s)} = 43(\mu W). \tag{2}$$

This leakage power mainly comes from the $0.9F$ supercapacitor used for StoreCap. By characterizing this StoreCap alone, its leakage power is approximated to 30μW.

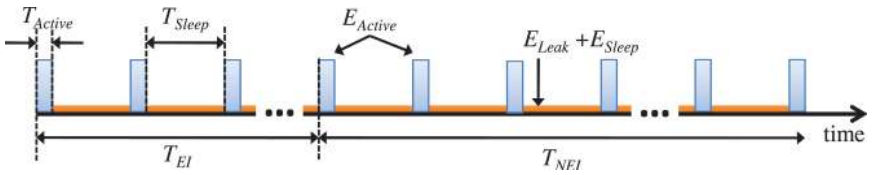

Fig. 7. Communications of the WSN node during a cycle of the periodic source. Harvested energy is only available during the harvesting energy interval (T_{EI}) instead of non-harvesting energy interval (T_{NEI}).

Therefore the total leakage power of the remaining components in MESC, including OutCap, the energy flow controller, and the comparator, is approximated to 13μW.

The DC/DC converter TPS61030 used in this work has an efficiency range between 80% to 93%. Unfortunately, its efficiency at a given time not only depends on the input voltage but also on the output current. Therefore it is impractical to achieve the efficiency precisely, as the input voltage from OutCap usually changes due to environmental conditions and because the output current depends on activities of the WSN node (transmission, reception, or sensing). Therefore the average DC/DC converter efficiency (η) is characterized in our design model. Two different scenarios with the same PowWow WSN node [Berder and Sentieys 2010] are set up to evaluate η. In the first scenario, the power supply of the node (V_{dd}) is directly connected to V_{OUT} without using the DC/DC converter. In the second one, V_{dd} is connected to the output of the DC/DC converter. The average consumed energy for both scenarios is 830μJ and 971μJ, respectively. As a consequence, $\eta = 0.85$. This obtained value is closer to the minimum (80%) than the maximum efficiency (93%) due to a small impact of the paradox issue.

5. ENERGY-NEUTRAL DESIGN FRAMEWORK

In this section, the implications of MESC when used as a plug-in for a practical energy harvesting WSN node are considered. In particular, the energy buffer size (C_{OUT} and C_{STORE}) and the estimation of system QoS at the design phase are discussed.

First of all, we present how to efficiently determine the size of OutCap (C_{OUT}). For a complete booting of the WSN node from the exhaustion of energy, the buffered energy in OutCap must satisfy the constraint

$$\frac{\eta}{2} C_{OUT}\left(V_{THR}^2 - V_{THF}^2\right) > E_{Reset}, \tag{3}$$

where E_{Reset} is the energy consumed by the WSN node during the booting process. The booting process is enabled as soon as V_{OUT} reaches V_{THR}. An amount of consumed energy E_{Reset} causes the voltage drop of V_{OUT}. However, V_{OUT} must be higher than V_{THF} for a successful booting. Eq. (3) means that energy buffered in C_{OUT} from voltage level V_{THF} to V_{THR} must be sufficient for the booting process.

Once the system has booted, the WSN node periodically performs communication in the active period (T_{Active}) and then stays in low-power mode during the sleep period (T_{Sleep}) as shown in Figure 7. Therefore T_{Sleep} can be considered as the QoS of the system. The lower T_{Sleep}, the better QoS. The size of C_{STORE} to maximize QoS, or to minimize T_{Sleep}, depends on the behavior of harvesting sources, the consumed energy, as well as the harvested energy. Let us show their relations in the following sections.

5.1. Periodic Energy Sources

In this section, it is assumed that the energy source is only harvested during a harvesting energy interval (T_{EI}) but not during a non-harvesting energy interval (T_{NEI}) (e.g., solar energy in an outdoor environment). This behavior is periodically repeated.

A technique to estimate T_{EI} and T_{NEI} can be found in Castagnetti et al. [2012]. Figure 7 shows one cycle of the periodic energy source where the WSN node is required to send data each T_{Sleep} during the whole cycle. Therefore, during the T_{EI}, a part of the harvested energy must be reserved in StoreCap for activities of the wireless node during T_{NEI}. The total harvested energy buffered in StoreCap during T_{EI} is estimated as

$$E_{EI} = P_H T_{EI} - \frac{1}{\eta}\left(\frac{T_{EI}}{T_{Sleep}} E_{Active} + P_{Sleep} T_{EI}\right) - P_{Leak} T_{EI}, \tag{4}$$

where P_H is the harvested power, T_{EI}/T_{Sleep} the number of wake-up times during T_{EI}, E_{Active} the consumed energy of the WSN node for each wake-up, P_{Sleep} the consumed power in sleeping mode, and P_{Leak} the leakage power of the whole system. The first term is the harvested energy during the energy interval, while the second one represents the consumed energy of the WSN node including active and sleeping periods. The total sleep time of the node during a harvesting energy interval is approximated to T_{EI} because T_{Active} (in order of *ms*) is negligible compared to T_{Sleep} (in order of *s*). Finally, total leakage energy is estimated as $P_{Leak} T_{EI}$. In order to buffer this amount of energy (E_{EI}), the size of StoreCap must satisfy

$$\frac{1}{2} C_{STORE}\left(V_{Max}^2 - V_{THF}^2\right) > E_{EI}, \tag{5}$$

where V_{Max} is the maximum voltage of the StoreCap. Meanwhile, the consumed energy during T_{NEI} is

$$E_{NEI} = \frac{1}{\eta}\left(\frac{T_{NEI}}{T_{Sleep}} E_{Active} + P_{Sleep} T_{NEI}\right) + P_{Leak} T_{NEI}. \tag{6}$$

To achieve theoretical infinite lifetime of the WSN node, the ENO condition after a cycle including T_{EI} and T_{NEI} needs to be satisfied. For this, we must have $E_{EI} = E_{NEI}$, and so

$$T_{Sleep} = \frac{(T_{EI} + T_{NEI})\, E_{Active}}{\eta P_H T_{EI} - (\eta P_{Leak} + P_{Sleep})(T_{EI} + T_{NEI})}. \tag{7}$$

This result presents the trade-off between the QoS of the system (T_{Sleep}), the consumed energy in the active period (E_{Active}), and the harvested power (P_H). Lower E_{Active} and higher P_H will increase system performance with a decrease of T_{Sleep}. Moreover, (4) and (5) present how C_{STORE} can be determined to maximize the QoS during the design phase. The increase of P_H requires more space in the StoreCap, otherwise a part of the harvested energy is discarded. Instead of having E_{EI}, only $\frac{1}{2} C_{STORE}(V_{Max}^2 - V_{THF}^2)$ can be used for operations during the non-harvesting energy interval (T_{NEI}). The QoS during T_{NEI} has to be reduced for ensuring the ENO condition and therefore it reduces the overall system QoS. It is interesting to notice that only the minimum C_{STORE} satisfying (5) provides the maximum QoS. Bigger capacitance would not improve the QoS due to higher leakage energy. Moreover, it is obvious that V_{STORE} at the end of a cycle should be equal to the value at the beginning of this cycle when ENO is satisfied. Unfortunately, the minimum V_{STORE} during a non-harvesting energy interval (T_{NEI}) is V_{THF}, which means that the ENO is only considered when $V_{STORE} > V_{THF}$ during the harvesting energy interval (T_{EI}). A simple solution is to charge V_{STORE} to V_{THF} before its deployment. Otherwise, the ENO cannot be satisfied until V_{STORE} reaches V_{THF}.

5.2. Continuous Energy Source

In constrast with the energy sources presented in the previous section, a continous energy source (e.g., heat energy from an industrial machine, light energy in a hospital)

usually provides harvested energy most of the time. A proposed WSN behavior when using this kind of energy source is that the WSN node always maximizes the QoS of the system without need for buffering energy in StoreCap. In this context, the ENO condition is only considered during the harvesting energy interval period. Therefore, from (4) and with $T_{NEI} = 0$, we have

$$T_{Sleep} = \frac{E_{Active}}{\eta\,(P_H - P_{Leak}) - P_{Sleep}}. \tag{8}$$

This result shows that the ENO condition is satisfied at any time of the energy interval because T_{Sleep} is independent of T_{EI}. As a consequence, the size of C_{STORE} is not important in this case because there is no surplus energy to charge the StoreCap. This behavior is also useful when C_{STORE} is fully charged ($V_{STORE} = V_{Max}$ in Figure 4). Since there is no more space for storing the harvested energy, the wireless node can maximize the QoS according to the harvested energy to avoid wasting energy. Moreover, (8) can be used to estimate the QoS of the system according to E_{Active} and P_H when the environmental energy is available.

Our design framework presents a trade-off to design an efficient MESC for a particular sensor node. It is obvious that when energy is only available for a certain period, a harvesting node has to buffer a part of harvested energy for continuous operation during the next non-harvesting energy interval. Therefore, the size of supercapactior must be optimized not only to sufficiently buffer the harvested energy but also to minimize the leakage energy. However, when harvested energy is available most of the time, the ENO operations of a harvesting node consist in consuming energy as much as it can harvest. In this context, a smaller size of StoreCap provides a better QoS due to the lower leakage. The next section shows in detail how capacitors are optimized when MESC is used for powering a PowWow WSN node.

6. EXPERIMENTAL RESULTS

6.1. Measurements Setup and C_{OUT} Sizing

In order to validate the design framework, experiments are performed using the PowWow WSN platform [Berder and Sentieys 2010] which is based on the MSP430 microcontroller and the CC2420 RF transceiver. MESC is configured to provide $V_{Re} = 3.3$V. The comparator is designed to provide $V_{THR} = 2.9$V and $V_{THF} = 1.8$V. The maximum voltage which is allowed for C_{STORE} is set to $V_{Max} = 5$V. $T_{EI} = 36000$s and $T_{NEI} = 50400$s for a typical winter day in our office environment.

For communications among nodes, asynchronous protocols have shown their energy efficiency for a low-traffic EH WSN [Bachir et al. 2010]. These protocols are based on a nonscheduled preample sampling that saves wasted energy due to the synchronization between many nodes. Some typical protocols in this field are RICER (*receiver-initiated cycled receiver*) [Lin et al. 2004], TICER (Transmitter Initiated Cycled Receiver) [Lin et al. 2004], WiseMAC (*wireless sensor MAC*) [El-Hoiydi and Decotignie 2004], and TAD-MAC (*traffic-aware dynamic MAC*) [Alam et al. 2012]. A meticulous choice of MAC protocol is key to improve the QoS of EH WSNs due to its direct impacts on the consumed energy (E_{Active}). TAD-MAC was shown to be an ultra-low-power and energy-efficient protocol for wireless body area sensor networks. Therefore it can be used for a single-hop EH WSN with a low variation on the wake-up period of many nodes. Meanwhile, WiseMAC is able to deal with the variation in a multihop network by exploiting knowledge of the schedule of neighbor nodes to provide a minimized preamble sampling. In a general network, either RICER or TICER can be used. For ensuring data transmission, the preamble must be long enough to have a successful rendez-vous.

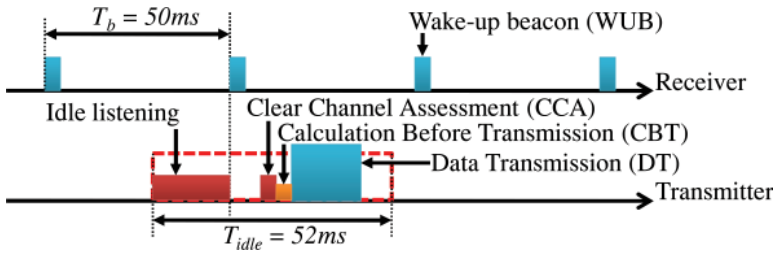

Fig. 8. Communication protocol between two nodes. When waking up, the transmitter waits for a *wake-up beacon* (WUB) from the receiver. After receiving a WUB, the transmitter forwards data packet (DT) after *clear channel assessment* (CCA) and *calculation before transmission* (CBT).

Table I. Energy Consumption of PowWow [Alam et al. 2011]

	Symbol	Value
Calculation Before Transmission	E_{CBT}	9.7μJ
Transmit/Receive wake-up Beacon	E_{WUB}	51μJ
Data Transmission	E_{DT}	80μJ
Data Reception	E_{DR}	100μJ
Clear Channel Assessment	E_{CCA}	18μJ
Transmission power	P_{Tx}	66.33mW
Reception power	P_{Rx}	76.89mW
Sleep power	P_{Sleep}	85.8μW

In this work, a simple MAC protocol based on RICER [Lin et al. 2004] illustrated in Figure 8 is used. This protocol has been validated on the PowWow platform and the energy consumed by the different states of the protocol stack was fully characterized [Alam et al. 2011]. The receiver, powered by batteries and connected to a host computer, sends a *wake-up beacon* (WUB) each $T_b = 50$ms. When a transmitter wants to send a data packet, it has to wait for a WUB from the receiver (idle listening). After receiving the WUB, the transmitter performs a *clear channel assessment* (CCA), *calculation before transmission* (CBT), and a *data packet transmission* (DT). In order to deal with clock drift, the maximum idle listening period at the transmitter is extended to 52ms. Acknowledgement packets (ACKs) are not used in this protocol as retransmission is not implemented at the transmitter. To evaluate the average consumed energy for each wake-up of the node, Table I (summarizing the consumed energy of each state) is used. For a long time measurement, we consider $T_{idle} = T_b/2$ as the average idle listening time, and therefore

$$E_{Active} = P_{Rx}T_{idle} + E_{WUB} + E_{CCA} + E_{CBT} + E_{DT} = 2081\mu J. \quad (9)$$

To determine C_{OUT}, the consumed energy for booting a PowWow node (E_{Reset}) has been experimentally estimated to 1094μJ. Therefore, from (3), C_{OUT} must be at least greater than 560μF. From the list of available capacitors and also to provide fault tolerance, a low-leakage 680μF capacitor is used for the OutCap.

6.2. Fast Booting Capability

Figure 9 shows the booting process with extracted data from a LeCroy oscilloscope when a PowWow node is powered by two PVs of size 4x6cm and is set up in our office (the light condition is around 400lux). At the begining, both C_{OUT} and C_{STORE} are empty. When PVs are connected to the PowWow node, V_{OUT} is rapidly increased. As soon as V_{OUT} reaches $V_{THF} = 2.9$V, the EN signal is enabled to power the node. There is a voltage drop on V_{OUT} due to the consumed energy process. However, V_{OUT} is still

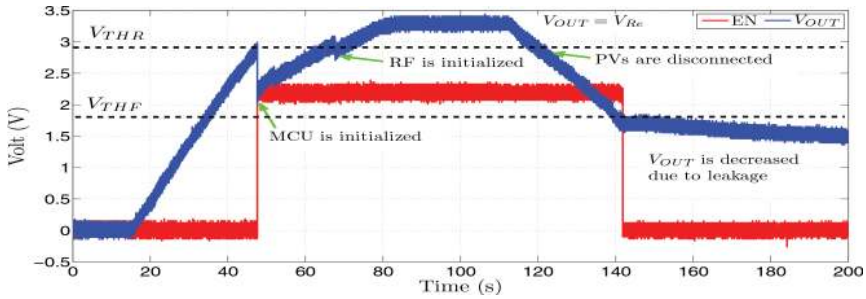

Fig. 9. Booting process with light energy in an office.

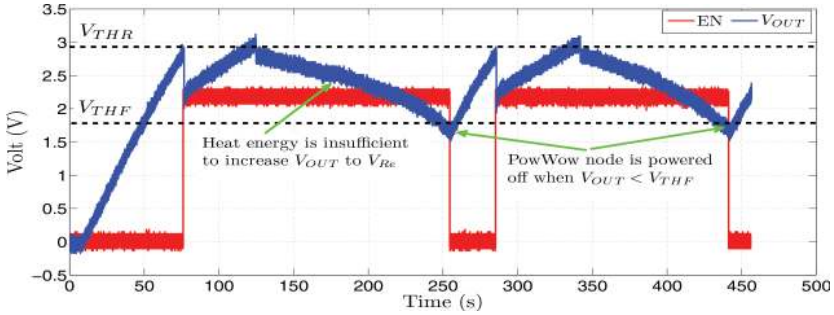

Fig. 10. V_{OUT} with thermal energy. After initializing the RF transceiver, the thermal energy is only enough to charge V_{OUT} to V_{Re}. More harvested power is required to satisfy the ENO of the EH WSN node.

higher than $V_{THF} = 1.8$V. From this point, the MCU stays in low-power mode and wakes up every 4s to read V_{OUT} through a low-powered ADC channel. As can be seen in Figure 9, V_{OUT} is more slowly increased when the node has booted, since a part of harvested energy is consumed by the MCU. Until V_{OUT} is higher than V_{RF}, the RF chip can be initialized to successfully complete the booting process. If a bigger capacitance is used for V_{OUT}, the booting time is longer due to the delay to charge V_{OUT} to V_{THF}. By using (3), we can optimize C_{OUT} to minimize the booting time, which is about 64s for both MCU and RF in this measurement.

Another promising energy source is the heat energy from industrial machines. WSNs with thermal energy can be used for monitoring the health condition of these machines. By analyzing their temperature, vibration, strain, and pressure in real time, engine maintenance will not be required until these data show it is necessary (rather than being regularly scheduled), therefore saving a great deal of cost. A TEG of size 30x30x3.3mm is used in this study. The hot surface is attached to a laptop adapter as the heat source while the cold surface is chosen to provide the heat spreading effect towards a heat sink. The temperature gap between the working PC adapter and the ambient air provides around 30mV output by the TEG. Figure 10 shows the voltage of the OutCap when a PowWow node is used with a TEG. Due to lower harvested energy, a longer booting time is required compared to a solar-powered node. After about 80s, the MCU is powered-on when $V_{OUT} = V_{THR}$. V_{OUT} keeps increasing as the harvested energy is still greater than the consumed energy of the PowWow node, which is at this time only the energy required by the MSP430. However, after initializing the CC2420 RF transceiver, the harvested energy is less than the total consumed energy of the node including both MSP430 and CC2420. Therefore V_{OUT} slightly decreases instead of continuously increasing to V_{Re}. After about 250s, the PowWow node is

Table II. Booting Time for Different EH WSN Platforms

Platform	Storage	Booting time
Heliomote	ThinEnergy 1.7mAh 4.1V	1830s ≈ 31min
Prometheus	CapXX 0.9F + ThinEnergy 1mAh 4.1V	1682s ≈ 28min
DuraCap	680μF +CapXX 1.8F	13s
MESC	680μF +CapXX 1.8F	17s

completely powered-off when $V_{OUT} = V_{THF}$. The node wakes up again when there is enough buffered energy in the OutCap until its next shutdown. Although the booting process is successful, heat energy in this measurement is insufficient to satisfy ENO. An obvious solution is to add one more TEG to improve the input power [Le et al. 2013].

To illustrate the fast booting capability of MESC, a simulation on OMNET++ is performed with three different platforms: Heliomote, Prometheus, and DuraCap. As these platforms are designed for outdoor applications, their original storage elements are too big (NiMH 1250mAh in Heliomote, 22F + NiMH 200mAh in Prometheus, and 50F + 250F in DuraCap) for a fair comparison. Therefore, their storage devices have been replaced to get a capacity roughly equivalent to MESC, which uses CapXX 1.8F for C_{STORE} and can store up to $1/2(C_{STORE}V_{Max}^2) = 22.5$J (energy in $C_{OUT} = 680\mu$F is negligible and $V_{Max} = 5$V). Therefore, a ThinEnergy 1.7mAh 4.1V battery (25J) is selected for Heliomote and a combination of CapXX 0.9F and ThinEnergy 1mAh 4.1V (22.3J) is used for Prometheus. Meanwhile, DuraCap, which is a dual-path architecture, has the same storage capacity as our MESC (680μF + CapXX 1.8F). As can be observed from Table II, Prometheus and Heliomote, which are based on the single-path architecture, require up to 1830s and 1682s, respectively, to charge their storage to at least 1.8V for powering our PowWow WSN node. The booting time is significantly reduced in DuraCap and MESC (13s and 17s, respectively) as both of them use the dual-path architecture. DuraCap has a better booting time since it is equipped with an MPPT to extract more light energy than our MESC in the same condition. However, MESC keeps the advantage of having different harvesters, instead of only PVs as in DuraCap. In this simulation, the light condition is around 1200lux that in results in a better booting time of MESC compared to real measurement shown in Figure 9 (64s at 400lux).

6.3. Energy-Neutral Design Framework Validation

In this section, measurements to validate the design framework with two kinds of energy sources are presented. The PowWow node is now powered by two PVs of size 4x6cm located in our office where the light condition is around 800lux. The harvested power at this condition is 574μW an average and can be considered as a periodic energy source. Therefore, from (7), $T_{Sleep} = 52$s. Figure 11 shows a short measurement of V_{STORE} when $T_{EI} = 1000$s and $T_{NEI} = 2000$s. As can be observed, the energy saved in the first 1000s is enough for the next 2000s. If a higher QoS is required, either more energy must be scavenged (e.g., bigger PVs) or the consumed energy during the active period (E_{Actice}) must be reduced.

Fluorescent light conditions in a hospital or an industrial environment are a potential energy source for monitoring applications using energy harvesting WSNs. This kind of energy source can provide a theoretical infinite T_{EI} because the indoor lights are usually switched on all the time. Therefore it can be considered as a continuous energy source. Considering the two PVs used in the previous measurement and applying (8) to simulate this situation, T_{Sleep} is reduced to 5.7s. Figure 12 presents the V_{STORE} of two different nodes when considering solar energy from two PVs as a nonperiodic source. V_{STORE} is almost constant because, from (8), the ENO condition is always

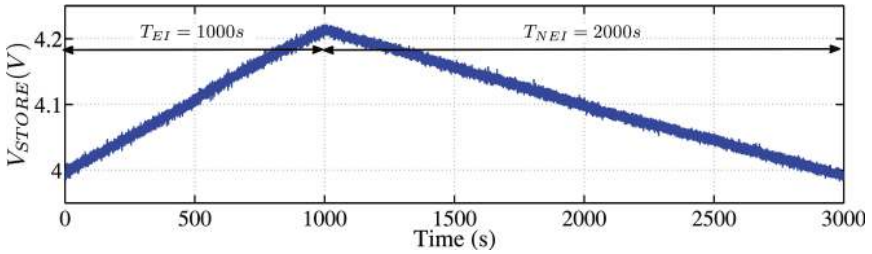

Fig. 11. V_{STORE} of a PowWow node powered by two PVs when $T_{Sleep} = 52$s. The harvested energy buffered in the first part (T_{EI}) is used in the second part when environmental energy is not available (T_{NEI}).

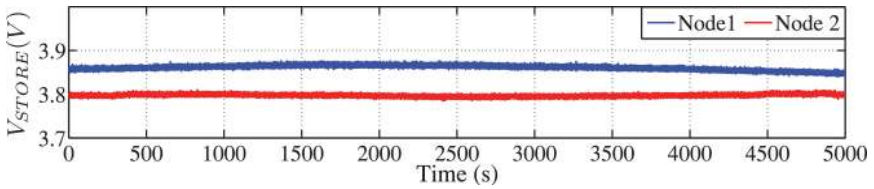

Fig. 12. V_{STORE} of two different PowWow nodes when $T_{Sleep} = 5.7$s. V_{STORE} stays nearly constant when two nodes have to follow the ENO condition.

satisfied. Experimental results presented in Figures 11 and 12 show the high accuracy of our system design model as the behavior of the node exactly satisfies the proposed application and the ENO condition.

6.4. Maximizing QoS in ENO

In this section, our energy-neutral design framework is used to determine C_{STORE} in order to maximize the QoS in ENO of the WSN node. The leakage power of the whole system is modeled by

$$P_{Leak} = 13 + \frac{C_{STORE}}{0.9F} 30(\mu W). \tag{10}$$

The leakage power of C_{STORE} is linearly increased with its capacitance and modeled based on the leakage power of the CapXX 0.9F characterized in Section 3. Meanwhile, leakage power of the remaining components of MESC is estimated to 13μW.

First of all, from (7) for a periodic energy source, the harvested power must be at least greater than 500μW to achieve a valid value of T_{Sleep} (the denominator must be greater than zero). Lower harvested power would not satisfy the ENO condition. In this context, harvested energy is less than the total consumed energy even if the WSN node always stays in sleeping mode without any communication. Figure 13 presents the average T_{Sleep} according to different levels of harvested power (P_H) and capacitance of the storage (C_{STORE}). As can be observed with $P_H = 600\mu$W, when $C_{STORE} =$ 0.9F, from (7), the wake-up period during T_{EI} can be reduced to 23s. Unfortunately, the condition (5) is false, the C_{STORE} is fully charged to V_{Max}, and then all of harvested energy is discarded. To ensure ENO, the performance during T_{NEI} (when there is no more harvested energy) must be reduced to 49s. Therefore the average wake-up period is only 33s as shown in Figure 13. When the size of C_{STORE} is increased to 1.1F, the system has more space to store the harvested energy and the wake-up period during T_{NEI} can be reduced to 28s. However, due to higher leakage, the performance during T_{EI} is reduced to 25s and therefore the average wake-up period of the WSN node is 27s. In this case, there is just a small part of harvested energy that

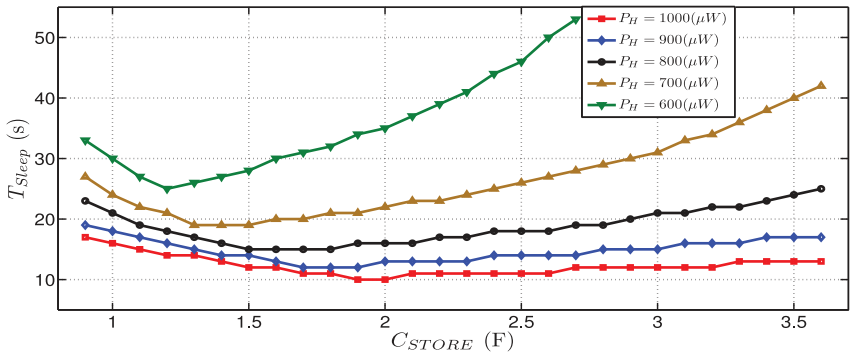

Fig. 13. Average wake-up period (T_{Sleep}) according to different harvested power (P_H) and storage capacitance (C_{STORE}) when considering a periodic energy source.

is wasted. The maximized performance with minimum wake-up period is achieved ($T_{Sleep} = 25$s) when $C_{STORE} = 1.2$F. All harvested energy is stored in the storage and used for packet transmissions. Increasing the size of C_{STORE} greater than 1.2F is not useful as the global consumed energy is also increased and the wake-up period has to increase to satisfy ENO. Although there is no wasted harvested energy when $C_{STORE} =$ 2F, the overall QoS ($T_{Sleep} = 35$s) is still lower than the case when $C_{STORE} = 0.9$F ($T_{Sleep} = 33$s).

When the harvested power is increased, the average wake-up period is reduced to provide better QoS as presented in Figure 13. For each level of harvested power, there is an optimized C_{STORE} which provides the highest QoS with minimum T_{Sleep}. However, the impact of leakage energy on the average wake-up period is reduced with high harvested power. When $P_H = 1000\mu$W (the red curve in Figure 13), the minimum T_{Sleep} is 10s when $C_{STORE} = 1.9$F. However, when C_{STORE} is increased to 3.6F, T_{Sleep} is only increased to 13s. From the datasheet of a harvester, its generated power can be estimated, and from our design framework, an optimized capacitance can be determined to maximize the system QoS while respecting the ENO condition.

A network simulation is constructed in OMNET++ with a harvested energy profile extracted from two PVs in size of 4x6cm located near a window in our office. A transmitter, which is an EH WSN node, sends a data packet every wake-up period to a receiver which is a permanent-powered WSN node. The protocol depicted in Figure 8 is implemented for their communication. The average power from PVs is estimated to $800\mu W$. From results in Figure 13, the maximum QoS can be achieved when $C_{STORE} =$ 1.8F and $T_{Sleep} = 15$s. As explained in Section 5.1, the start-up voltage of the V_{STORE} should be greater than $V_{THF} = 1.8$V to satisfy the ENO condition with a periodic energy source. V_{STORE} is initialized to 2V to provide fault tolerance.

Figure 14 presents V_{STORE} when the wake-up period of the WSN node (T_{Sleep}) is fixed to 15s during the whole simulation. It is worth noting that during the first half of a day (from around 8:00am to 12:00am), due to outdoor solar radiance, the harvested energy is higher than the second half of the day, when there is only indoor fluorescent light. It is observed that the ENO condition is well satisfied in the first day. Harvested energy is sufficiently buffered during the harvesting energy interval (working hours) for perpetual operation during the non-harvesting energy interval (night hours). After a day, which is also a cycle for this energy source, V_{STORE} is closely recovered to its initial voltage. The next two days present a positive energy error when the harvested energy is greater than the consumed energy (the second day), and a negative energy

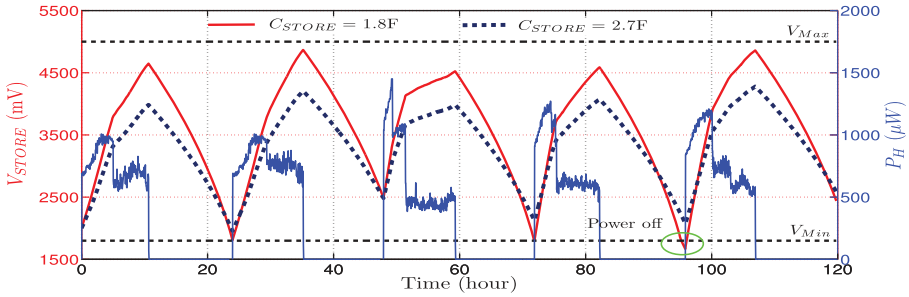

Fig. 14. V_{STORE} of an EH WSN node with different values of C_{STORE} in OMNET++ simulation. C_{STORE} = 1.8F not only provides higher QoS (T_{Sleep} = 15s) but also better efficiency (93.86% of C_{STORE} is used) compared to 2.7F (T_{Sleep} = 19s and 81.91% of C_{STORE} is used).

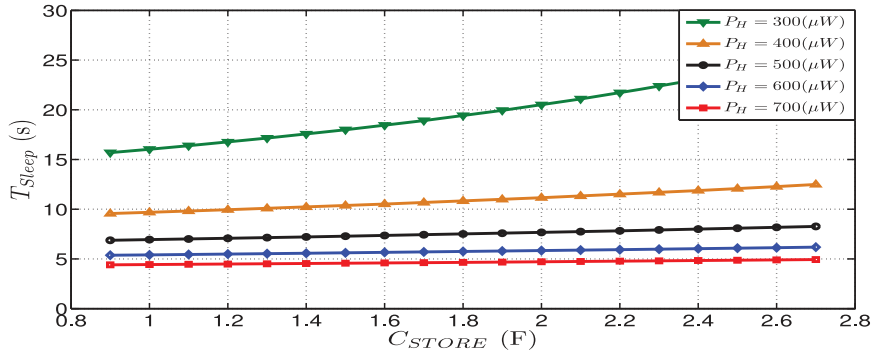

Fig. 15. Average wake-up period (T_{Sleep}) according to different harvested power (P_H) and storage capacitance (C_{STORE}) when considering a continuous energy source.

error when the harvested energy is less than the consumed energy (the third day). The wake-up period in the second day should be lower than 15s and, vice versa, higher than 15s in the third day. During a short period (about 20 minutes) at the end of the fourth day the WSN node is completely powered-off when $V_{STORE} < V_{THF}$, and therefore no more packets can be sent to the receiver during this interval. The most interesting result from this simulation is the efficient sizing of C_{STORE}. On average, 93.86% of C_{STORE} is utilized with a small free space. Increasing the size of C_{STORE} not only increases the free space, which is a hardware cost, but also reduces the system QoS due to higher leakage. This simulation is restarted again with C_{STORE} composed of three 0.9F capacitors in parallel (2.7F). As can be observed in Figure 14, only 81.91% of C_{STORE} is used and T_{Sleep} is reduced to 19s. However, with higher capacitance, C_{STORE} in this simulation provides better fault tolerance and therefore V_{STORE} is still higher than V_{THF} at the end of the fourth day for continuous operations.

For a continuous energy source, the harvested power must be greater than 200μW to satisfy the ENO. As can be observed from Figure 15, the leakage energy due to bigger capacitance has a linear impact on the wake-up period of the node. This problem has been presented in Le et al. [2013] where a *duty-cycle power manager* (DC-PM) adapts the wake-up period of a thermal-powered PowWow node in real time. The average performance is reduced about 1s when two 0.09F capacitors, instead of only one, are used for C_{STORE}. However, the wake-up period is more stable with higher capacitance since the DC-PM does not regard small changes on V_{STORE}, which is the main input to perform adaptations. In the contrast, with lower capacitance, the DC-PM is more

sensitive to the change of V_{STORE}, which results in more variation of the wake-up period. This behavior should be taken into account with the design of MAC protocol. For instance, TAD-MAC requires a stable wake-up of the transmitter to optimize the wake-up period of the receiver. Meanwhile, WiseMAC is able to deal with variations of the wake-up period. Finally, the impact of leakage energy is also reduced with higher energy from the harvester.

7. CONCLUSION

Energy harvesting techniques have been considered as a potential solution to design an autonomous WSN with a theoretically infinite lifetime. In this article, the *multiple-energy-sources converter* (MESC), compatible with different environmental sources, is proposed. Exploiting the advantages of a dual-path architecture for EH WSNs, our MESC can power a WSN node after only 17s from an empty energy state instead of 28 and 31 minutes for Prometheus and Heliomote, respectively. Although supercapacitors provide durable energy storage, their leakage can degrade the global QoS of the WSN node. Therefore, the main contribution in this article is a precise energy-neutral design framework which provides various considerations for an efficient energy harvesting WSN, such as the size of energy storage (C_{OUT} and C_{STORE}) to maximize the QoS of the system according to the consumed energy, and the harvested energy when following the ENO condition. Simulation results show that up to 93.86% capacity of C_{STORE} derived from our design framework is used, significantly reducing the cost of the redundancy and leakage energy. Future work will focus on a *dynamic power manager* (DPM) adapting the QoS according to harvested energy from a periodic energy source such as the light energy in an office environment. In this context, the DPM will have to buffer energy during the harvesting energy interval for continuous operation during the non-harvesting energy interval.

ACKNOWLEDGMENTS

The authors would like to thank Samuel Mouget and Romain Fontaine for their design PCB and support.

REFERENCES

I. F. Akyildiz, W. Su, Y. Sankarasubramaniam, and E. Cayirci. 2002. Wireless sensor networks: A survey. *J. Comput. Netw.* 38, 4, 393–422.

M. M. Alam, O. Berder, D. Menard, T. Anger, and O. Sentieys. 2011. A hybrid model for accurate energy analysis of WSN nodes. *EURASIP J. Embedd. Syst. 2011,* 1–16.

M. M. Alam, O. Berder, D. Menard, and O. Sentieys. 2012. TAD-MAC: Traffic-aware dynamic MAC protocol for wireless body area sensor networks. *IEEE J. Emerg. Select. Topics Circ. Syst.* 2, 109–119.

A. Bachir, M. Dohler, T. Watteyne, and K. K. Leung. 2010. MAC essentials for wireless sensor networks. *IEEE Comm. Surv. Tutor.* 12, 2, 222–248.

S. Bandyopadhyay and A. P. Chandrakasan. 2012. Platform architecture for solar, thermal, and vibration energy combining with MPPT and single inductor. *IEEE J. Solid-State Circ.* 47, 9, 2199–2215.

O. Berder and O. Sentieys. 2010. PowWow: Power optimized hardware/software framework for wireless motes. In *Proceedings of the International Conference on Architecture of Computing Systems (ARCS'10).* 1–5.

D. Carli, D. Brunelli, L. Benini, and M. Ruggeri. 2011. An effective multi-source energy harvester for low power applications. In *Proceedings of the Design, Automation and Test in Europe Conference and Exhibition (DATE'11).* 1–6.

D. Carli, D. Brunelli, D. Bertozzi, and L. Benini. 2010. A high-efficiency wind-flow energy harvester using micro turbine. In *Proceedings of the International Symposium on Power Electronics Electrical Drives Automation and Motion (SPEEDAM'10).* 778–783.

E. J. Carlson, K. Strunz, and B. P. Otis. 2010. A 20 mV input boost converter with efficient digital control for thermoelectric energy harvesting. *IEEE J. Solid-State Circ.* 45, 4, 741–750.

A. Castagnetti, A. Pegatoquet, C. Belleudy, and M. Auguin. 2012. A framework for modeling and simulating energy harvesting WSN nodes with efficient power management policies. *EURASIP J. Embedd. Syst. 2012,* 8, 1–16.

C. Y. Chen and P. H. Chou. 2010. DuraCap: A supercapacitor-based, power-bootstrapping, maximum power point tracking energy-harvesting system. In *Proceedings of the International Symposium on Low Power Electronics and Design (ISLPED'10).* 313–318.

P. H. Chou and C. Park. 2005. Energy-efficient platform designs for real-world wireless sensing applications. In *Proceedings of the IEEE/ACM International Conference on Computer-Aided Design (ICCAD'05).* 913–920.

A. El-Hoiydi and J. D. Decotignie. 2004. WiseMAC: An ultra low power MAC protocol for multi-hop wireless sensor networks. In *Proceedings of the 1st International Workshop on Algorithmic Aspects of Wireless Sensor Networks (ALGOSENSORS'04).* 18–31.

T. Esram and P. L. Chapman. 2007. Comparison of photovoltaic array maximum power point tracking techniques. *IEEE Trans. Energy Convers.* 22, 2, 439–449.

N. Ferry, S. Ducloyer, N. Julien, and D. Jutel. 2013. Power and energy aware design of an autonomous wireless sensor node. *J. Adv. Comput. Sci.* 2, 4, 11–36.

M. E. Glavin, P. K. W. Chan, S. Armstrong, and W. G. Hurley. 2008. A stand-alone photovoltaic supercapacitor battery hybrid energy storage system. In *Proceedings of the 13th Power Electronics and Motion Control Conference (EPE-PEMC'08).* 1688–1695.

T. He, S. Krishnamurthy, L. Luo, T. Yan, L. Gu, R. Stoleru, G. Zhou, Q. Cao, P. Vicaire, J. A. Stankovic, T. F. Abdelzaher, J. Hui, and B. Krogh. 2006. VigilNet: An integrated sensor network system for energy-efficient surveillance. *ACM Trans. Sensor Netw.* 2, 1, 1–38.

M. Y. I. Idris, E. M. Tamil, N. M. Noor, Z. Razak, and K. W. Fong. 2009. Parking guidance system utilizing wireless sensor network and ultrasonic sensor. *J. Inf. Technol.* 8, 2, 138–146.

X. Jiang, J. Polastre, and D. Culler. 2005. Perpetual environmentally powered sensor networks. In *Proceedings of the International Symposium on Information Processing in Sensor Networks (IPSN'05).* 463–468.

A. Kansal, J. Hsu, S. Zahedi, and M. B. Srivastava. 2007. Power management in energy harvesting sensor networks. *ACM Trans. Embedd. Comput. Syst.* 6, 4.

S. Kim and P. H. Chou. 2011. Energy harvesting by sweeping voltage-escalated charging of a reconfigurable supercapacitor array. In *Proceedings of the International Symposium on Low-Power Electronics and Design (ISLPED'11).* 235–240.

T. N. Le, A. Pegatoquet, O. Sentieys, O. Berder, and C. Belleudy. 2013. Duty-cycle power manager for thermal-powered wireless sensor networks. In *Proceedings of the IEEE Symposium on Personal, Indoor and Mobile Radio Communications (PIMRC'13).* 1655–1659.

E. Y. A. Lin, J. M. Rabaey, and A. Wolisz. 2004. Power-efficient rendez-vous schemes for dense wireless sensor networks. In *Proceedings of the IEEE International Conference on Communications (ICC'04).* 3769–3776.

C. Liu, K. T. Chau, and X. Zhang. 2010. An efficient wind-photovoltaic hybrid generation system using doubly excited permanent-magnet brushless machine. *IEEE Trans. Industr. Electron.* 57, 3, 831–839.

F. Ongaro, S. Saggini, and P. Mattavelli. 2012. Li-ion battery-supercapacitor hybrid storage system for a long lifetime, photovoltaic-based wireless sensor network. *IEEE Trans. Power Electron.* 27, 9, 3944–3952.

C. Park and P. H. Chou. 2006. AmbiMax: Autonomous energy harvesting platform for multi-supply wireless sensor nodes. In *Proceedings of the 3rd Annual IEEE Communications Society Conference on Sensor and Ad Hoc Communications and Networks (SECON'06).* 168–177.

V. Raghunathan, A. Kansal, J. Hsu, J. Friedman, and M. Srivastava. 2005. Design considerations for solar energy harvesting wireless embedded systems. In *Proceedings of the International Symposium on Information Processing in Sensor Networks (IPSN'05).* 463–468.

F. J. Rincon, M. Paselli, J. Recas, Z. Qin, M. Sanchez-Elez, D. Atienza, J. Penders, and G. De Micheli. 2008. OS-based sensor node platform and energy estimation model for health-care wireless sensor networks. In *Proceedings of the Design, Automation and Test in Europe Conference (DATE'08).* 1027–1032.

D. Salerno. 2010. Ultralow voltage energy harvester uses thermoelectric generator for battery-free wireless sensors. *LT J. Analog Innovat.* 20, 3, 1–11.

F. I. Simjee and P. H. Chou. 2008. Efficient charging of supercapacitors for extended lifetime of wireless sensor nodes. *IEEE Trans. Power Electron.* 23, 3, 1526–1536.

A. M. Sommariva. 2003. Solving the two capacitor paradox through a new asymptotic approach. *IEE Proc. Circ. Devices Syst.* 150, 2, 227–231.

M. Stordeur and I. Stark. 1997. Low power thermoelectric generator-self-sufficient energy supply for micro systems. In *Proceedings of the International Conference on Thermoelectrics (ICT'97).* 575–577.

C. K. Tse, S. C. Wong, and M. H. L. Chow. 1995. On lossless switched-capacitor power converters. *IEEE Trans. Power Electron.* 10, 3, 286–291.

T. Zhu, Z. Zhong, Y. Gu, T. He, and Z. L. Zhang. 2009. Leakage-aware energy synchronization for wireless sensor networks. In *Proceedings of the International Conference on Mobile Systems, Applications, and Services (MobiSys'09)*. 319–332.

Received December 2013; revised June 2014; accepted August 2014